ELSEVIER

1 February 1998

Optics Communications 147 (1998) 196–202

OPTICS COMMUNICATIONS

Full length article

Performance of an optical fiber butt-coupled Cr^{3+}:$LiSrAlF_6$ laser

Nilesh J. Vasa [a,1], Husayin Parhat [a], Tatsuo Okada [a], Mitsuo Maeda [a], Osamu Uchino [b]

[a] *Graduate School of Information Science and Electrical Engineering, Kyushu University, Hakozaki, Fukuoka 812-81, Japan*
[b] *Division of Meteorological Satellite and Observation System, Meteorological Research Institute, Tsukuba, Ibaraki 305, Japan*

Received 4 August 1997; revised 7 October 1997; accepted 8 October 1997

Abstract

Pumping of a Cr^{3+}:LiSAF laser through a butt-coupled optical fiber is investigated for a compact all-solid-state laser assembly. Theoretical space-dependent rate equation analysis is used to predict the output characteristics of the Cr^{3+}:LiSAF laser for different cavity parameters, optical fiber characteristics, and Cr^{3+} doping rates. The effect of the positional and angular mismatch of the pump beam with respect to the laser mode is also included in the model. The analysis explicitly shows that the slope efficiency can be improved by improving the mode coupling volume in the Cr^{3+}:LiSAF crystal. Experimental output characteristics are reported when the Cr^{3+}:LiSAF laser is pumped through optical fibers with different combinations of core diameter and numerical aperture. The experimental results are in good agreement with the theoretical modeling. © 1998 Elsevier Science B.V.

PACS: 42.55.R; 42.60.B; 42.60.D

Keywords: Tunable laser; Cr^{3+}:LiSAF laser; Fiber-coupled pumping; Laser analysis

1. Introduction

Cr^{3+}-doped $LiSrAlF_6$ (Cr^{3+}:LiSAF) possesses a combination of spectrally broad absorption and emission cross sections. It has a gain bandwidth extending from ≈ 750 to 1000 nm [1]. The main attractive feature of this medium is that part of the broad absorption band (600–700 nm) matches the commercially available InGaAlP red diode laser. Therefore recently there is a growing interest in developing compact all-solid-state tunable Cr^{3+}:LiSAF laser sources [2–6]. Most of the investigations reported by many researchers so far have used conventional pumping optics for coupling a pump beam to the Cr^{3+}:LiSAF crystal.

There is one more possible configuration of pumping the Cr^{3+}:LiSAF crystal by directly butt-coupling an optical fiber to the crystal. Pumping of different solid-state lasers such as Nd:YAG and Nd:YVO_4 lasers through butt-coupled optical fibers has been demonstrated by various research groups [7–9]. Compared to the Cr^{3+}:LiSAF crystal, the Nd:YAG crystal has higher fluorescence lifetime, and the Nd:YVO_4 crystal has higher stimulated emission cross section as well as higher absorption coefficient. Further, in the Cr^{3+}:LiSAF laser, the upper-state lifetime quenching is also a critical factor as a result of the increase of temperature at the pump spot [10–15]. Due to this thermal quenching problem, with a butt-coupled optical fiber, the circular pump beam is expected to limit an efficient scaling towards very high input powers as compared to the arrangement consisting of an asymmetric pump beam in a vertically thin crystal [11–13] and pumping both ends of the crystal. However, the advantage of using the butt-coupled optical fiber is that it allows a more compact and simple construction by eliminating pump collimating and focusing optics between the fiber end and laser crystal pump end. In addition, with a similar configuration, a fiber grating can also be used with a grating

[1] E-mail: vasa@laser.ed.kyushu-u.ac.jp.

PII S0030-4018(97)00598-1

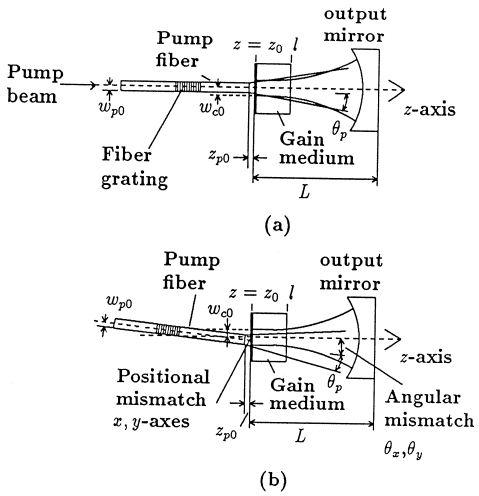

Fig. 1. Configuration of the Cr^{3+}:LiSAF laser pumped through the directly coupled optical fiber. (a) When the pump fiber is properly aligned, hence the pump beam and laser mode are collinear. (b) When the pump fiber is in a misaligned position resulting in pump beam positional and angular mismatch with respect to the laser mode.

formed on the same fiber where the fiber grating forms a part of the Cr^{3+}:LiSAF laser coupled-cavity as shown schematically in Fig. 1. The fiber grating can provide a narrow-band feedback at a Bragg wavelength corresponding to the Cr^{3+}:LiSAF laser wavelength for spectral narrowing operation of the Cr^{3+}:LiSAF laser [6], and the pump beam can also be transmitted through the same fiber. Thus it can permit the use of a single-frequency tunable microchip assembly without any intracavity tuning elements.

Further, many authors have theoretically investigated the influence of the laser and pump mode sizes on the laser output characteristics with a conventional coupling optics [16–24]. However, in the case where an optical fiber is directly butt-coupled to the lasing medium, not only the pump beam divergence, but spatial and angular misalignment are also very critical factors affecting the output characteristics due to pump and laser mode overlap integral.

In this work, first, a space-dependent rate equation analysis for cw laser operation is considered to deal with pumping the Cr^{3+}:LiSAF crystal through the directly butt-coupled optical fiber. The output characteristics is evaluated based on the laser mode and pump beam coupling volume with a linear approximation of the output versus input power equation. The dependence of the threshold power and output characteristics on different cavity parameters such as spot size of the laser mode, pump beam radius, pump beam position, pump beam divergence, spatial and angular mismatch between the pump beam and laser mode axes, different Cr^{3+} doping rates of the Cr^{3+}:LiSAF media is investigated. Subsequently, experimental study on the output characteristics of a Cr^{3+}:LiSAF laser when pumped by a directly coupled optical fiber (pump fiber) is carried out. In the experiment, pump fibers with different combinations of core diameter and numerical aperture were considered. The theoretical and experimental results are compared to understand the effectiveness of the arrangement.

2. Theoretical modeling

2.1. Model and formulation

Fig. 1 shows the configuration for pumping a Cr^{3+}:LiSAF crystal through a directly coupled optical fiber model. Fig. 1(a) shows the properly aligned condition of the pump beam with respect to the laser mode, while Fig. 1(b) represents positional and angular misalignment. Based on the space-dependent rate equation analysis [16,19,21], the threshold power requirement and the relationship between input and output power can be derived with a similar approach and can be expressed as follows,

$$P_{\mathrm{th}} = \frac{\sigma_{\mathrm{e}}\gamma I_{\mathrm{s}}}{2\eta_{\mathrm{p}}(\sigma_{\mathrm{e}} - \sigma_{\mathrm{esa}})} \frac{1}{\int_{\mathrm{cavity}} gm \,\mathrm{d}V}, \tag{1}$$

where P_{th} is the threshold power input, σ_{e} is the stimulated emission cross section, γ is the total logarithmic loss $(2\alpha_{\mathrm{c}} l + T)$, α_{c} is the distributed loss per unit length, l is the crystal length, T is the transmission loss, η_{p} is the pump efficiency $(\nu_{\mathrm{l}}/\nu_{\mathrm{p}})$, ν_{l} is and ν_{p} are the laser and pump frequencies respectively, σ_{esa} represents loss in the gain cross section due to excited state absorption, I_{s} is the saturation intensity $(h\nu_{\mathrm{l}}/\sigma_{\mathrm{e}}\tau)$, $h\nu_{\mathrm{l}}$ is the energy of the laser photon, τ is the upper state lifetime, g and m represent the normalized pump and normalized laser mode distributions inside the active medium respectively, and $\int_{\mathrm{cavity}} gm \,\mathrm{d}V$ represents the effective spatial overlapping of the pump and laser mode distributions.

$$P_{\mathrm{out}} = \frac{T\eta_{\mathrm{p}}}{\gamma} \frac{(\sigma_{\mathrm{e}} - \sigma_{\mathrm{esa}})}{\sigma_{\mathrm{e}}} (P_{\mathrm{in}} - P_{\mathrm{th}}) \frac{\left[\int_{\mathrm{cavity}} gm \,\mathrm{d}V\right]^2}{\int_{\mathrm{cavity}} gm^2 \,\mathrm{d}V}, \tag{2}$$

where P_{out} is the laser output power, $(\int_{\mathrm{cavity}} gm \,\mathrm{d}V)^2/\int_{\mathrm{cavity}} gm^2 \,\mathrm{d}V$ represents the factor affecting the overlapping efficiency and it is termed mode-coupling factor ('mcf'). Thus the slope efficiency is the product of the coupling efficiency $\eta_{\mathrm{c}} = T/\gamma$, pump efficiency η_{p}, the factor due to excited-state absorption $(\sigma_{\mathrm{e}} - \sigma_{\mathrm{esa}})/\sigma_{\mathrm{e}}$, and mode-coupling factor 'mcf'.

The integrations in Eqs. (1) and (2) can be solved numerically to yield the output characteristics. In general, for a focused pump beam geometry using conventional optics, the mathematical analyses can be simplified further by assuming constant pump and laser mode beam radius and considering a collinear pump and laser mode beam geometry in the gain medium. However with directly butt-coupled fiber pumping, these assumptions are not appropriate since pump beam distributions, pump beam divergence as well as spatial and angular alignment of the pump beam with respect to the laser mode also affect the output characteristics.

In case of a multi-mode fiber, the pump beam at the output end of the fiber is similar to a super-Gaussian distribution of high order. Therefore the pump beam distribution is assumed to be a top-hat distribution. The normalized pump beam distribution g including the effect of spatial and angular mismatch can be given by

$$g = \frac{\alpha_p}{\pi w_p^2(z)} \exp(-\alpha_p z)\, \theta\Big(w_p(z) - \sqrt{(x_p + \theta_x z - x_i)^2 + (y_p + \theta_y z - y_i)^2}\Big), \quad (3)$$

where α_p is the absorption coefficient, z is the distance from the crystal input end, (x_p, y_p) is the center of the pump beam due to spatial misalignment at the crystal input end, θ_x and θ_y represent angular mismatch, (x_i, y_i) is the x and y coordinate of the cell i, $\theta(w_p(z) - \sqrt{(x_p + \theta_x z - x_i)^2 + (y_p + \theta_y z - y_i)^2})$ is the Heaviside step function, and $w_p(z)$ is the spot size along the z axis and assumed to propagate according to

$$w_p(z) = w_{p0} + \theta_p(z_{p0} + z/n_p), \quad (4)$$

where w_{p0} is the pump spot size at the fiber exit end which corresponds to the fiber core diameter, θ_p is the far-field half-angle of the pump beam based on the numerical aperture NA of the fiber, z_{p0} is the distance of the fiber exit end from the crystal input end, and n_p is the refractive index corresponding to the pump wavelength.

Considering single transverse mode TEM_{00} laser operation, m is given by

$$m = \frac{2}{\pi w_m^2(z)} \exp\left(-2\frac{(x_m - x_i)^2 + (y_m - y_i)^2}{w_m^2(z)}\right), \quad (5)$$

where (x_m, y_m) is the center of the laser mode at the crystal input end, and $w_m(z)$ is the laser mode spot size along the z axis and assumed to propagate according to

$$w_m^2(z) = w_{c0}^2\left\{1 + \frac{(z - z_{m0})^2 \lambda_m^2}{\pi^2 w_{c0}^4 n_m^2}\right\}, \quad (6)$$

where w_{c0} is the laser mode spot size at the beam waist, i.e. at z_{m0} position, λ_m is the laser mode wavelength and n_m is the refractive index of the crystal corresponding to the laser mode wavelength.

Further, in a very general form, the output characteristics can also be evaluated by calculating the output efficiency ϕ_{out}. The output efficiency ϕ_{out} is nothing but the ratio of output power to input power and can be expressed as

$$\phi_{out} = P_{out}/P_{in}. \quad (7)$$

By substituting Eqs. (1) and (2) into Eq. (7), the following expression for the output efficiency ϕ_{out} is obtained,

$$\phi_{out} = \frac{T\eta_p}{\gamma}\frac{\sigma_e - \sigma_{esa}}{\sigma_e}\left[1 - \frac{\sigma_e \gamma I_s}{2\eta_p(\sigma_e - \sigma_{esa})P_{in}}\right] \times \frac{1}{\int_{cavity} gm\, dV}\left[\frac{\left[\int_{cavity} gm\, dV\right]^2}{\int_{cavity} gm^2\, dV}\right]. \quad (8)$$

The output efficiency ϕ_{out} can be used for evaluating the optimum operating condition for laser operation.

2.2. Model predictions

Eqs. (1) and (2) are solved numerically to observe the influence of different cavity parameters on threshold power P_{th} requirements and mode-coupling factor 'mcf'. The numerical calculations are performed by dividing the total volume of the Cr^{3+}:LiSAF crystal into small cuboidial cells, each having a square cross section of 1 μm^2 in the transverse direction and a length of 25 μm in the longitudinal direction. The values of some of the standard parameters used throughout the calculations are listed in Table 1.

First, an effect of pump beam position z_{p0} with respect to the crystal end along the z direction is considered. The best position is obtained when z_{p0} is equal to zero, i.e. when the pump fiber is perfectly butt coupled to the crystal.

Table 1
Numerical values for standard parameters used in the analysis

Description	Symbol	Numerical values
Pump wavelength	λ_p	679 nm
Laser wavelength	λ_c	830 nm
Absorption coefficient	α_p	
1.5 at.% doped		10 cm^{-1}
3 at.% doped		20 cm^{-1}
Fluorescence lifetime	τ	67 μs [25]
Refractive index – at λ_p	n_p	1.4094 [26]
Refractive index – at λ_c	n_c	1.4076 [26]
Stimulated emission cross section	σ_e	4.8×10^{-20} cm^2 [27]
ESA cross section	σ_{esa}	1.6×10^{-20} cm^2 [27]
Output mirror transmission	T	0.02
Distributed loss per unit length	α_c	0.015 cm^{-1} [28,29]

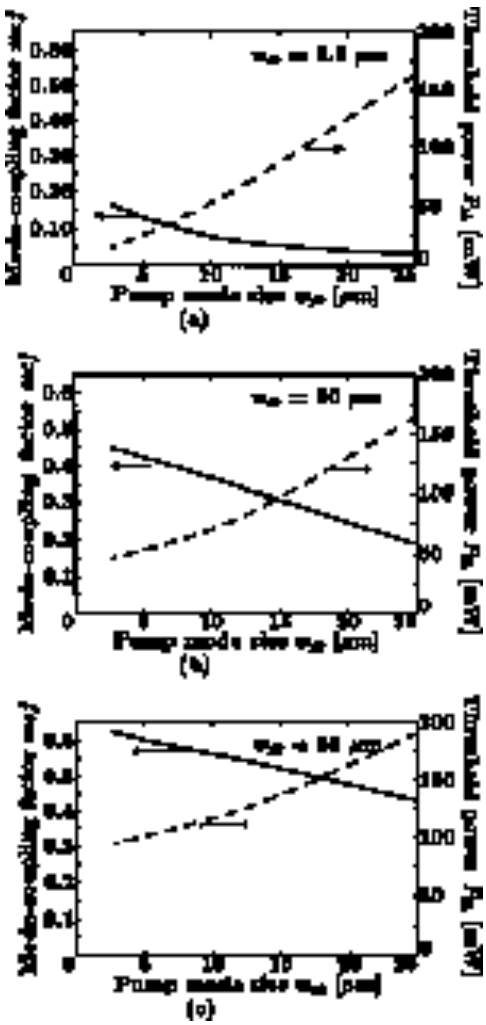

Fig. 2. Threshold power P_{th} and mode-coupling factor 'mcf' as function of pump beam size w_{p0} for different values of laser mode waist w_{c0}. (a) w_{c0} = 5 μm, (b) w_{c0} = 20 μm, (c) w_{c0} = 35 μm. Numerical aperture NA of pump fiber = 0.12. Dahed line corresponds to the threshold power P_{th} requirement and solid line corresponds to the mode coupling factor 'mcf'.

Fig. 2(a), 2(b) and 2(c) show plots of threshold power P_{th} and mode-coupling factor 'mcf' as a function of the pump beam size w_{p0} for the laser mode waist w_{c0} with typical values of 5 μm, 20 μm and 35 μm respectively. In the calculation, the pump beam is assumed to be collinear with the laser mode and z_{p0} is equal to zero. The results show that for a given laser mode size, the smaller the pump size the lower the threshold value and the higher the mode-coupling factor 'mcf' representing the higher overlap. Further as shown in Fig. 2(a), 2(b) and 2(c), the mode-coupling factor 'mcf' can be improved by increasing the laser mode size w_{c0}, but at the expense of increase of threshold power P_{th}. Thus the best tradeoff in terms of the

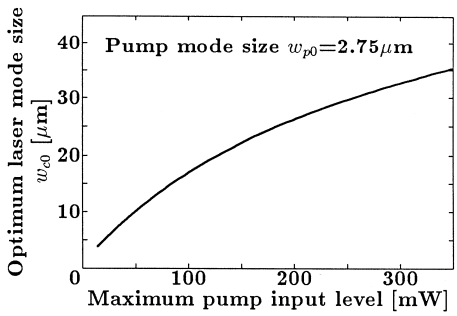

Fig. 3. Optimum value of laser mode size w_{c0} for different input pump levels. Numerical aperture NA of pump fiber = 0.12. Optimum value is calculated to attain maximum output efficiency.

output power depends on the input power level and an optimum value of the laser mode size can be expected with a maximum of the output efficiency ϕ_{out}. The numerical calculation of Eq. (8) is performed to determine the optimum value of the laser mode size w_{c0} for different input power levels. In the calculation, the pump fiber of core diameter of 5.5 μm and NA of 0.12 is considered. Fig. 3 shows the optimum value for the laser mode size for different input power. The optimum laser mode size value is an increasing function of the input power, eventhough the threshold power P_{th} requirement also increases with increase of laser mode size as shown in Fig. 2.

Fig. 4 shows the effect of numerical aperture NA of the pump fiber and hence the effect of the pump beam divergence angle θ_p on the threshold power P_{th} and the mode-coupling factor 'mcf'. In case of multi-mode fibers, the transmitted pump beam follows the beam divergence corresponding to the NA of the pump fiber. As NA increases, the far-field pump beam divergence also increases and in turn, the propagation angle of the beam along the z axis can be too large to allow good overlap with the laser mode. Thus, an optimum slope efficiency can be obtained

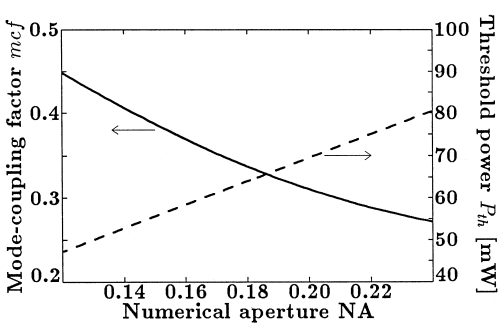

Fig. 4. Influence of optical fiber numerical aperture NA i.e. pump beam divergence angle on output characteristics of the Cr^{3+}:LiSAF laser. w_{c0} = 20 μm and w_{p0} = 2.75 μm. Dashed line corresponds to the threshold power P_{th} requirement and solid line corresponds to the mode coupling factor 'mcf'.

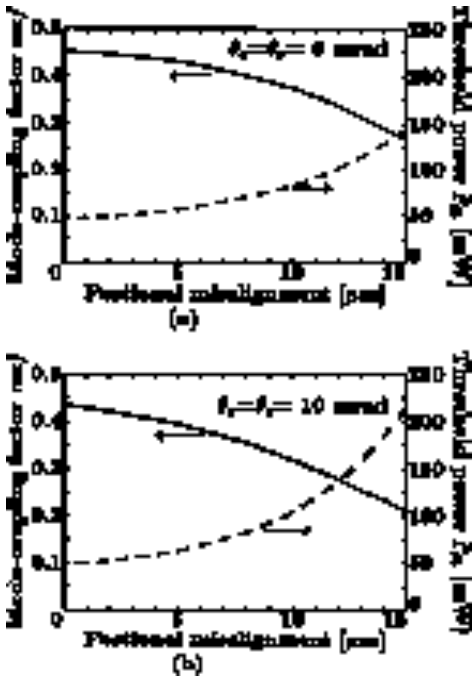

Fig. 5. Effect of positional misalignment and angular mismatch between pump mode and laser mode on output characteristics of the Cr^{3+}:LiSAF laser. $w_{c0} = 20$ μm and $w_{p0} = 2.75$ μm. (a) Without angular deviation, (b) with angular deviation of 10 mrad. Dashed line corresponds to the threshold power P_{th} requirement and solid line corresponds to the mode coupling factor 'mcf'.

with minimum NA and minimum pump beam size. On the other hand, in case of a single-mode fiber corresponding to the pump beam, under an equilibrium condition the transmitted pump beam will be a Gaussian pump beam. Hence the overlapping efficiency is decided in a similar way to that of conventional Gaussian optics.

Fig. 5 shows the dependence of the Cr^{3+}:LiSAF laser output characteristics on positional and angular mismatch of the pump mode with respect to the laser mode. Fig. 5(a), 5(b) shows the effect of positional mismatch without angular deviation and with angular deviation of $\theta_x = \theta_y = 10$ mrad, respectively. The positional mismatch corresponds to positional deviation in transverse directions at the pump input end and in the calculations measurement across the diagonal is considered. The angular mismatch corresponds to the angular deviation of the pump mode propagating along the z axis. Fig. 5 shows that as the positional or the angular mismatch increases, the threshold power P_{th} increases and the mode-coupling factor 'mcf' decreases. This adverse effect is due to decrease of the mode overlapping volume which is responsible for transferring the power between the pump mode and laser mode. The calculation explicitly shows that pump beam alignment is a critical factor which affects the output characteristics.

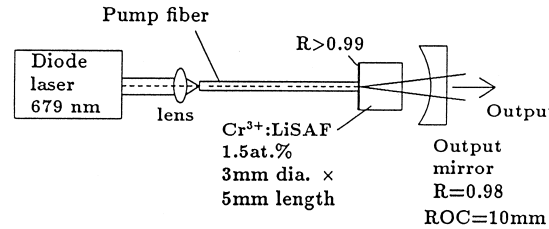

Fig. 6. Experimental setup.

3. Experimental results and discussion

A 1.5 at.% doped Cr^{3+}:LiSAF crystal (3 mm diameter × 5 mm length) was considered in the experiment. Fig. 6 shows the experimental setup. The pump end of the crystal was coated for high reflectivity at the laser wavelength. An output coupler of radius of curvature (ROC) 10 mm and with a reflectivity of 98% was used. As a pump source, a diode laser (679 nm, SDL-7350-A6) was focused into a pump fiber through a lens (Melles Griot 06 GLC 003) and the pump fiber was directly butt-coupled to the Cr^{3+}:LiSAF crystal. Precautions were taken for not to maintain any gap between the pump fiber end and the crystal. Three different pump fibers; Fiber A (core diameter 50 μm, NA 0.2), Fiber B (core diameter 9.3 μm, NA 0.12), and Fiber C (core diameter 5.5 μm, NA 0.12) were considered and the output characteristics of the Cr^{3+}:LiSAF laser were measured. In the experiment, corresponding to the pump wavelength of 679 nm, all the pump fibers were multi-mode fibers, however, Fiber C with a cut-off wavelength of 780 nm was a single-mode fiber corresponding to the lasing wavelength of the Cr^{3+}:LiSAF laser.

Fig. 7 shows the output characteristics of the Cr^{3+}:LiSAF laser when pumped through Fiber A, Fiber B and Fiber C. The solid curves in Fig. 7 represent the theoretical fitting and the solid circles represent the experi-

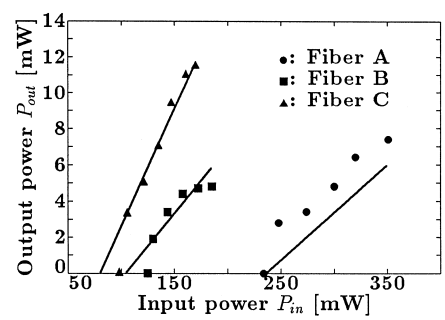

Fig. 7. Output characteristics of the Cr^{3+}:LiSAF laser when pumped through Fiber A, Fiber B and Fiber C. Solid curves represent theoretical fitting and solid marks represent experimental results. Fiber A: core diameter = 50 μm, NA = 0.2, Fiber B: core diameter = 9.3 μm, NA = 0.12, Fiber C: core diameter = 5.5 μm, NA = 0.12.

mental results. In the experiment, it was comparatively difficult to align the pump fiber perfectly collinear to the laser mode geometry. Further, since it was rather difficult, if not impossible, to carry out direct measurement of spatial and angular mismatch during the experiment, the experimental condition of spatial and angular mismatch between the pump and the laser mode was included in the calculations of Eqs. (1) and (2) using mismatch parameters f_1 and f_2,

$$P_{\text{th}} = \frac{\sigma_e \gamma I_s}{2\eta_p(\sigma_e - \sigma_{esa})} f_1 \frac{1}{\int_{\text{cavity}} gm \, dV}, \tag{9}$$

$$P_{\text{out}} = \frac{T\eta_p}{\gamma} \frac{(\sigma_e - \sigma_{esa})}{\sigma_e} (P_{\text{in}} - P_{\text{th}}) f_2 \frac{\left[\int_{\text{cavity}} gm \, dV\right]^2}{\int_{\text{cavity}} gm^2 \, dV}. \tag{10}$$

The mismatch parameter f_1 represents the deviation of effective spatial overlapping due to poor matching between the pump and the laser mode and influences the threshold power requirements, while the mismatch parameter f_2 represents the deviation of the mode-coupling factor affecting the overlapping efficiency. Threshold power requirements and slope efficiencies were calculated by using Eqs. (9) and (10), and fitted to the experimental data using the mismatch parameters f_1 and f_2. Fig. 7 shows that the theoretical prediction of the model agrees well with the experimental data. Table 2 lists the values of the mismatch parameters and theoretically calculated output characteristics for each fiber. It is explicit that as the fiber core diameter and the numerical aperture of the pump fiber are decreased, the output characteristics of the Cr^{3+}:LiSAF laser are improved. However, for Fiber B and Fiber C, the value of f_1 is on the higher side and the value of f_2 is on the lower side as compared to the value 1.0 for the perfect collinear overlapping of pump and laser modes. Thus higher threshold power requirement and lower slope efficiency values can be attributed to poor mode-matching conditions.

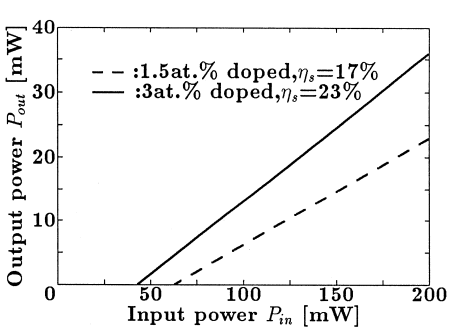

Fig. 8. Calculated optimum output characteristics of the Cr^{3+}:LiSAF laser when pumped through Fiber C (core diameter = 5.5 μm, NA = 0.12). Optimum laser mode size w_{c0} = 26 μm corresponding to maximum input level of 200 mW. Solid line represents 3 at.% doped crystal and dashed line represents 1.5 at.% doped crystal.

Table 2
Mode coupling data and calculated output characteristics

Description	Fiber A	Fiber B	Fiber C
Pump beam size w_{p0} [μm]	25	4.5	2.75
Pump beam full divergence [radian]	0.2	0.12	0.12
Laser mode size w_{c0} [μm]	22	20	20
Mode-coupling factor 'mcf' [ratio]	0.14	0.44	0.45
Fitted mismatch parameter f_1	1	2	1.7
Fitted mismatch parameter f_2	1	0.54	0.9
Threshold power P_{th} [mW]	235	104	80
Slope efficiency η_s [%]	5	7	13

Therefore it is worthwhile to note that, with an improvement in the pump beam and mode matching condition, the threshold power P_{th} requirement can be lowered and the slope efficiency η_s can be increased further. Fig. 8 shows the calculated output characteristics of the Cr^{3+}:LiSAF laser when the crystal is pumped through the Fiber C with the assumption that the pump beam and the laser mode are collinear, i.e. matching parameters f_1 and f_2 are considered to be equal to 1.0. The solid line shows output characteristics for a 3 at.% doped Cr^{3+}:LiSAF crystal, while the dashedline is for a 1.5 at.% doped Cr^{3+}:LiSAF crystal. In the calculation, the optimum laser mode size of 26 μm is considered for a typical maximum input level of 200 mW. With a 1.5 at.% doped crystal, the threshold power P_{th} is ≈ 63 mW and the slope efficiency η_s of 17% can be obtained. Further, improving the absorption characteristics per unit length of the crystal by increasing the doping rate to 3 at.%, the threshold power P_{th} requirement will decrease to 43 mW with an increase in the slope efficiency η_s to 23%. However, similar to a conventional arrangement for symmetric pump laser beam focusing, even with a butt-coupled optical fiber which has a round pump beam profile, the operation is expected to be limited in a low input–output power regime. This is mainly due to the upper-state lifetime quenching of the Cr^{3+}:LiSAF laser, as a result of high pump spot temperature, as compared to the optical arrangement consisting of asymmetric pump beam and lasing mode [11–13]. The adverse thermal effect related to decreasing lifetime and increasing upconversion problems will be more prominent with increasing Cr^{3+} doping rates [14].

4. Conclusion

Pumping of the Cr^{3+}:LiSAF laser through the butt-coupled fiber is attained, however the performance critically

depended on the fiber core size, numerical aperture of the fiber and the mismatch condition between the pump beam and the laser mode. A theoretical model, based on the space-dependent rate equation analysis, has been used to understand the influence of various cavity parameters. The effect of the spatial and angular mismatch between the pump beam and the laser mode is also included in the theoretical model. This model provides useful guidelines for designing an optimum Cr^{3+}:LiSAF laser when pumped through a butt-coupled fiber and it can also be applied to evaluate the performance of the other laser media. Experimental results are in good agreement with the predictions of the model. Further, based on the laser mode and the pump mode coupling calculations, the output characteristics can be improved with an optimum doping rate in the crystal and with an improved beam coupling efficiency. This configuration is expected to permit a very compact tunable-all-solid-state laser source with an external grating formed on the pump fiber, where the same fiber grating forms a part of the cavity for the Cr^{3+}:LiSAF laser.

Acknowledgements

We wish to thank Prof. T. Mizunami and Dr. S. Gupta of Kyushu Institute of Technology, for helpful discussions and for providing optical fibers with different characteristics for the experiment. We are also thankful to M. Kidosaki for extending his assistance in the experiment.

References

[1] M. Stalder, B.H.T. Chai, M. Bass, Appl. Phys. Lett. 58 (1991) 216.
[2] Q. Zhang, G.J. Dixon, B.H.T. Chai, P.N. Kean, Optics Lett. 17 (1992) 43.
[3] J.M. Sutherland, S. Ruan, R. Mellish, P.M.W. French, J.R. Taylor, Optics Comm. 113 (1995) 458.
[4] M. Ihara, M. Tsunekane, N. Taguchi, H. Inaba, Electron. Lett. 31 (1995) 888.
[5] R. Knappe, K.J. Boller, R. Wallenstein, Optics Lett. 20 (1995) 1988.
[6] N.J. Vasa, T. Okada, M. Maeda, T. Mizunami, O. Uchino, Optics Lett. 21 (1996) 1472.
[7] J.J. Zayhowski, J. Ochoa, C. Dil III, Digest of Conference on Lasers and Electro-optics-1995, pp. 139.
[8] A. Caprara, J. Henden, S. McDermott, D. Neklason, Digest of Conference on Lasers and Electro-optics-1995, pp. 173.
[9] J.J. Zayhowski, C. Dil III, Optics Lett. 20 (1995) 716.
[10] M. Stalder, M. Bass, B.H.T. Chai, J. Opt. Soc. Am. B 9 (1992) 2271.
[11] D. Kopf, K.J. Weingarten, L.R. Brovelli, M. Kamp, U. Keller, Optics Lett. 19 (1994) 2143.
[12] D. Kopf, K.J. Weingarten, G. Zhang, M. Moser, M.A. Emanuel, R.J. Beach, J.A. Skidmore, U. Keller, Appl. Phys. B 65 (1997) 235.
[13] D. Kopf, U. Keller, M.A. Emanuel, R.J. Beach, J.A. Skidmore, Optics Lett. 22 (1997) 99.
[14] N.P. Barnes, C.C. Johnson, D.J. Reichle, K.E. Murray, Digest of Conference on Lasers and Electro-optics-1997, pp. 257.
[15] F. Balembois, F. Falcoz, F. Kerboull, F. Druon, P. Georges, A. Brun, IEEE J. Quantum Electron. 33 (1997) 269.
[16] A.J. Alfrey, IEEE J. Quantum Electron. 25 (1989) 760.
[17] P.F. Moulton, IEEE J. Quantum Electron. 21 (1985) 1582.
[18] T.Y. Fan, R.L. Byer, IEEE J. Quantum Electron. 24 (1988) 895.
[19] W.P. Risk, J. Opt. Soc. Am. B 5 (1988) 1412.
[20] D.G. Hall, R.J. Smith, R.R. Rice, Appl. Optics 19 (1980) 3042.
[21] P. Laporta, IEEE J. Quantum Electron. 27 (1991) 2319.
[22] Y.F. Chen, T.S. Liao, C.F. Kao, T.M. Huang, K.H. Lin, S.C. Wang, IEEE J. Quantum Electron. 32 (1996) 2010.
[23] Y.F. Chen, C.F. Kao, S.C. Wang, Optics Comm. 133 (1997) 517.
[24] Y.F. Chen, T.M. Huang, K.H. Lin, C.F. Kao, C.L. Wang, S.C. Wang, Optics Comm. 136 (1997) 399.
[25] S.A. Payne, L.K. Smith, R.J. Beach, B.H.T. Chai, J.H. Tassano, L.D. DeLoach, W.L. Kway, R.W. Solarz, W.F. Krupke, Appl. Optics 33 (1994) 5526.
[26] S.A. Payne, W.F. Krupke, L.K. Smith, W.L. Kway, L.D. DeLoach, J.B. Tassano, IEEE J. Quantum Electron. 28 (1992) 1188.
[27] W.R. Rapoport, M.L. Shand, Solid State Commun. 84 (1992) 29.
[28] S.A. Payne, L.L. Chase, L.K. Smith, W.L. Kway, H.W. Newkirk, J. Appl. Phys. 66 (1989) 1051.
[29] N.J. Vasa, H. Sui, T. Okada, M. Maeda, X. Wu, O. Uchino, Mem. Fac. Eng., Kyushu Univ. 55 (1995) 115.